Journal of Organometallic Chemistry 694 (2009) 1840–1847

Contents lists available at ScienceDirect

Journal of Organometallic Chemistry

journal homepage: www.elsevier.com/locate/jorganchem

p-Diethynylbenzene-based molecular wires, *Fe*–C≡C-*p*-$C_6H_2X_2$–C≡C–*Fe* [*Fe* = Fe(η^5-C_5Me_5)(dppe)]: Synthesis, substituent effects and unexpected formation of benzodifuran complex

Yumi Matsuura, Yuya Tanaka, Munetaka Akita *

Chemical Resources Laboratory, Tokyo Institute of Technology, R1-27, 4259 Nagatsuta, Midori-ku, Yokohama 226-8503, Japan

ARTICLE INFO

Article history:
Received 11 November 2008
Received in revised form 12 January 2009
Accepted 13 January 2009
Available online 20 January 2009

Keywords:
Iron
Acetylide
Molecular wire
Substituent effects
Redox
X-ray crystallography

ABSTRACT

A series of *p*-diethynylbenzene-based molecular wires, *Fe*–C≡C-*p*-$C_6H_2X_2$–C≡C–*Fe* (**3**) (*Fe* = FeCp*(dppe)), is prepared and their wire-like performance is estimated on the basis of the K_C and V_{ab} values. It has been revealed that electron-donating substituents (X) improve the performance. The benzodifuran complex **4** unexpectedly formed from the derivative with X = OH shows the performance comparable to **3**.

1. Introduction

Organic π-conjugated systems combined with metal fragments have been studied from the viewpoint of molecular devices [1,2]. In particular, one-dimensional organometallic molecular wires with redox-active metal attachments have been studied most extensively [3–6], because the electron-donating metal end caps can stabilize the cationic radical species resulting from oxidation and furthermore their wire-like performance is conveniently evaluated on the basis of their electrochemical properties, K_C (comproportionation constant) for the 1e-oxidized, mixed valence species.

The organic π-conjugated parts can be constructed by a combination of a limited number of sp-(C≡C) and sp^2-hybridized hydrocarbyl components (e.g. C=C and phenylene). Of a variety of structural motifs of the linkers studied so far, polyynediyl bridges [$(C{\equiv}C)_n$] turn out to be superior to other bridges as revealed by the studies, in particular, using the highly electron-donating M($(\eta^5$-$C_5R_5)L_2$ fragments [M/L_2 = Fe/$(PR_3)_2$ [4], Ru/$(PR_3)_2$ [5], Re/(NO)(PR_3) [6]] (Scheme 1). The polyynediyl ligands, however, cannot be modified, because no substituent can be introduced onto the sp-hybridized carbon atoms. In a previous paper, we reported synthesis of a series of endiyne–diiron complexes, *Fe*–C≡C–C(R)=C(R)–C≡C–*Fe* [*Fe* = FeCp*(dppe)], and the substituent effects [7,8]. It is notable that some of the aryl-substituted derivatives show wire-like performance even superior to the polyynediyl complexes and thus the family of the complexes is regarded as "tunable molecular wires".

In order to further study substituent effects our research efforts were focused on a series of the *p*-diethynylbenzene derivatives, *Fe*–C≡C-*p*-$C_6H_2X_2$–C≡C–*Fe*. In addition to the major purpose, we attempted switching of the wire-like performance by introduction of pH-sensitive substituents (X = OH and NMe_2) [9]. Although the latter attempts were not always successful, a new π-conjugated polycyclic system, i.e. benzodifuran complex, resulted from the precursor with X = OH.

2. Results and discussion

2.1. Synthesis of *p*-diethynylbenzene-based molecular wires, *Fe*–C≡C-*p*-$C_6H_2X_2$–C≡C–*Fe* (*3*)

The *p*-diethynylbenzene derivatives **3** were prepared by the "vinylidene method" following the procedures reported for the parent compound **3d** by Lapinte (Scheme 2) [4d,g,o,10]. The solvated cationic FeCp*(dppe) species ([Cp*(dppe)Fe(MeOH)]$^+$), which was formed via ionization of *Fe*–Cl in MeOH in the presence of KPF_6, captured 1-alkyne to cause spontaneous isomerization to the vinylidene intermediate $\mathbf{2}^{2+}(PF_6)_2$. Subsequent deprotonation afforded the acetylide complexes **3** except for the OH derivative

* Corresponding author.
E-mail address: makita@res.titech.ac.jp (M. Akita).

0022-328X/$ - see front matter © 2009 Elsevier B.V. All rights reserved.
doi:10.1016/j.jorganchem.2009.01.019

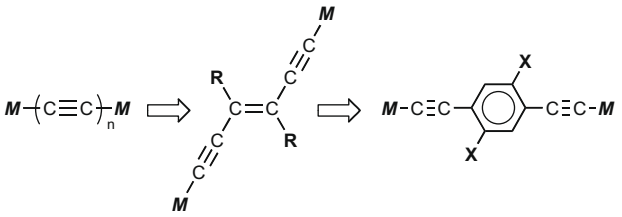

Scheme 1.

1g (see below) [11]. The obtained products **3** were sparingly soluble in common organic solvents, as reported for **3d** [4d], but readily characterized by spectroscopic features, in particular, on the basis of the ν(C≡C) vibrations and the simple NMR spectra containing single sets of signals for the aryl and *Fe* moieties in accord with the symmetrical structures.

For measurements of the IVCT bands (see below), the neutral compounds **3** were converted into the monocationic species $\mathbf{3}^{+}$ by treatment with $[FeCp_2]PF_6$ in CH_2Cl_2.

2.2. Formation of benzodifuran complex *4* and preparation of its S-analogue, benzodithiophene complex *5*

Reaction of the OH derivative **1g** with the Fe reagent did not afford the expected acetylide complex **3g** but the unexpected doubly fused benzodifuran complex **4** (Scheme 3). The red product **4** turned out to be an isomer of **3g** as judged by the ESI-MS data (m/z = 1334.8) but its IR spectrum did not contain an O–H vibration essential for the expected structure. Although **4** could not be characterized by its spectroscopic data alone, a clue to the structure was obtained from X-ray crystallography of the cationic intermediate $\mathbf{2}^{2+}\mathbf{g}'$ obtained by repeated recrystallization of a reaction mixture of the Fe reagent and **1g** [12; see also Section 3.4]. The cationic intermediate $\mathbf{2}^{2+}\mathbf{g}'$ was characterized as the dicationic Fischer-type cyclic di(O-substituted-carbene) species [13] with the doubly fused tricyclic structure, which should result from nuclephilic addition of the OH group at the electrophilic vinylidene α-carbon atom in $\mathbf{2}^{2+}\mathbf{g}$ followed by proton migration (Scheme 3). Action of a base to $\mathbf{2}^{2+}\mathbf{g}'$ should cause deprotonation from the methylene moieties to form the furan structures in **4**. For a comparison sake, the benzodithiophene complex **5**, an S-analogue of **4**, was prepared via a different route, i.e. reaction of lithiated benzodithiophene with I-FeCp(CO)$_2$ followed by photochemical ligand replacement with dppe (Scheme 3). The neutral compounds **4** and **5** were also converted into the monocationic species $\mathbf{4}^{+} \cdot PF_6$ and $\mathbf{5}^{+} \cdot PF_6$, respectively, by treatment with $[FeCp_2]PF_6$.

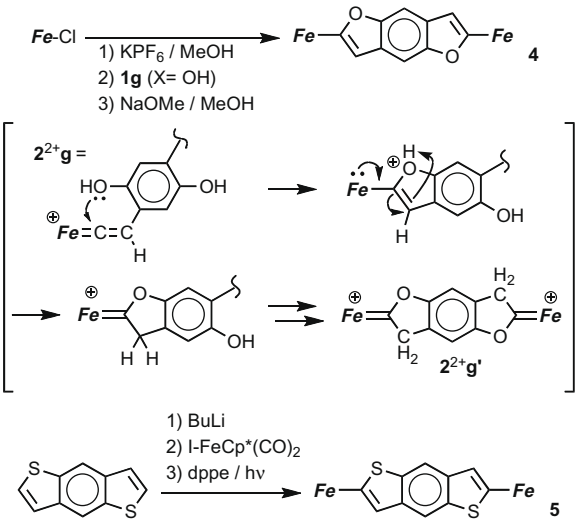

Scheme 3.

2.3. Evaluation of wire-like performance of complexes *3–5*

2.3.1. Electrochemical evaluation

In order to evaluate the performance of the obtained diiron complexes **3–5** as molecular wires they were subjected to CV measurements [14]. All monocationic *p*-diethynylbenzene species $\mathbf{3}^{+}$ showed two reversible redox waves separated by 250–330 mV (ΔE), as typically exemplified for $\mathbf{3}^{+}\mathbf{a} \cdot PF_6$ (Fig. 1a) [15]. The CV charts for the other derivatives are included in the Supporting Information (Fig. S1). From the ΔE values the comproportionation constants (K_C) are determined to be 2.2×10^4–4.3×10^5 (Table 1). The benzodifuran complex **4** and its S-analogue **5** show the K_C values comparable to those of **3**. The K_C values for complexes **3–5** fall in the range for those of class II Robin-Day compounds [16].

2.3.2. Near IR spectra

Monocationic species of high-performance molecular wires show an intense and broad IVCT (intervalence charge transfer) band in the near IR (NIR) region, and the V_{ab} value obtained from the spectrum is regarded as another measure for the performance as molecular wire, in case the monocationic species is isolable [17]. Although no theoretical relationship between the K_C and V_{ab} values is established, an efficient molecular wire shows larger K_C and V_{ab} values.

All monocationic species $\mathbf{3}^{+}$–$\mathbf{5}^{+}$ show intense NIR absorptions in the range of 3000–10000 cm^{-1}. A typical NIR spectrum for $\mathbf{3}^{+}\mathbf{a}$ is

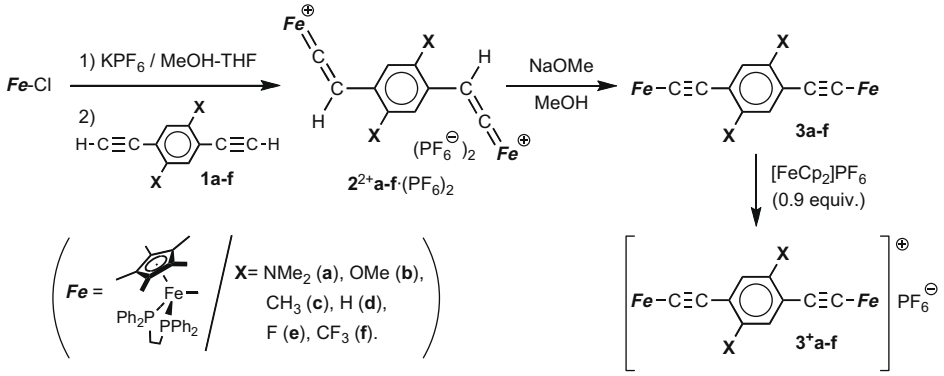

Scheme 2.

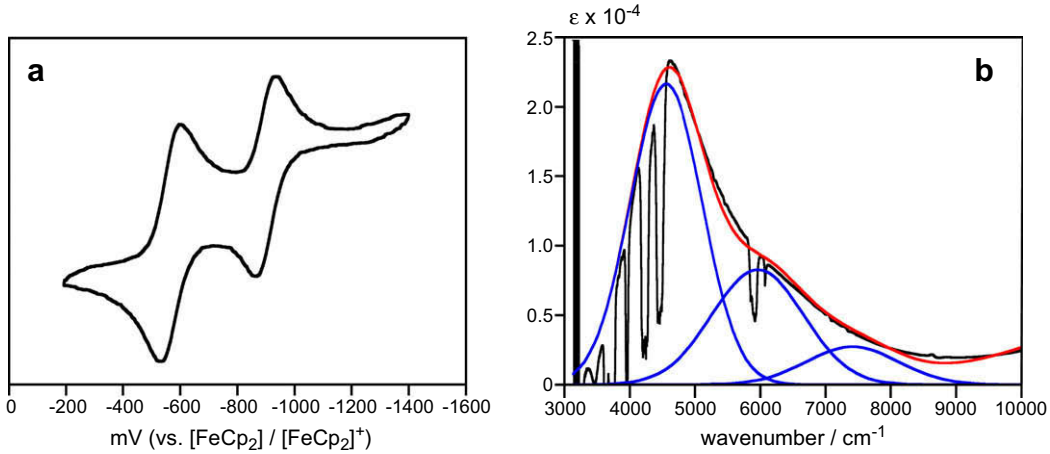

Fig. 1. (a) A cyclic voltammogram for $\mathbf{3}^{+}\mathbf{a}$ ([$\mathbf{3}^{+}\mathbf{a}\cdot PF_6$] = 2.0×10^{-3} M; [$Bu_4N\cdot PF_6$] = 0.1 M; Pt electrode; observed in CH_2Cl_2). (b) A NIR spectrum for $\mathbf{3}^{+}\mathbf{a}\cdot PF_6$ (observed in CH_2Cl_2; black: observed spectrum; blue: deconvoluted Gaussian curves; red: sum of the deconvoluted curves). (For interpretation of the references in color in this figure legend, the reader is referred to the web version of this article.)

Table 1
CV data for the diiron complexes **3**–**5**.[a]

Complex (X/σ_p)	E^1_c (mV)	E^1_a (mV)	$\lvert E^1_c - E^1_a\rvert$ (mV)	$E^1_{1/2}$ (mV)	E^2_a (mV)	E^2_c (mV)	$\lvert E^2_c - E^2_a\rvert$ (mV)	$E^1_{1/2}$ (mV)	ΔE (mV)	i_{c1}/i_{a1}	i_{c2}/i_{a2}	K_C
3a (NMe_2/−0.83)	−935	−867	68	−901	−602	−535	67	−569	333	1.0	1.0	4.3×10^5
3b (OMe /−0.27)	−869	−802	67	−836	−559	−492	67	−526	310	1.0	1.0	1.8×10^5
3c (Me/−0.07)	−835	−769	66	−802	−554	−487	67	−520	282	0.9	1.1	5.9×10^4
3d (H/0)	−792	−728	64	−760	−536	−472	64	−504	256	1.1	1.0	2.2×10^4
3e (F/0.06)	−739	−673	66	−706	−451	−387	64	−419	287	0.8	0.8	7.2×10^4
3f (CF_3/0.54)	−704	−639	65	−672	−409	−347	62	−378	294	1.1	1.0	9.5×10^4
4	−1020	−932	88	−976	−675	−597	78	−636	340	1.0	1.0	5.7×10^5
5	−890	−777	113	−834	−634	−525	109	−580	254	0.9	0.9	2.0×10^4

[a] Observed in CH_2Cl_2; [complex] = ; [NBu_4PF_6] = 0.1 M; Pt electrode; the values are reported with respect to the $FeCp_2/[FeCp_2]^+$ couple.

shown in Fig. 1b. (Spectra for the other derivatives are included in the Supporting Information (Fig. S2 and Table S1) [18]). The absorptions appear in the lower energy region so that they overlap with the solvent absorptions (CH_2Cl_2). Deconvolution analysis revealed that the NIR absorptions can be analyzed as a sum of three Gaussian curves [17]. Of the NIR absorptions the most intense bands of the lowest energies were assigned to the IVCT bands [17], and the V_{ab} values were obtained on the basis of their spectral parameters (Table 2).

The V_{ab} value for class II Robin-Day compounds can be calculated according to the Hush formula: $V^{II}_{ab} = 2.55\times10^{-6}\ (\nu_{max}\cdot\varepsilon\cdot\nu_{1/2})^{1/2}r^{-1}$ (in eV), where ν_{max}, ε, $\nu_{1/2}$, and r denote the absorption maximum, absorption coefficient, half-height width, and distance between the two redox active centers, respectively [16]. On the other hand, for class III Robin-Day compounds, for which the half-height width ($\nu_{1/2}$) is narrower than the critical value $(2310\nu_{max})^{1/2}$ (in cm^{-1}), the electronic coupling can be evaluated using the equation $V^{III}_{ab} = 1/2\nu_{max}$ (in cm^{-1}) = $6.20\times10^{-5}\ \nu_{max}$ (in eV) [16].

The spectral parameters and the obtained V_{ab} values are summarized in Table 2 (see also Table S1). The V^{II}_{ab} and V^{III}_{ab} values fall in the ranges of 0.01–0.08 and 0.25–0.34, respectively. For all compounds, the $\nu_{1/2}$ values are smaller than the critical values, suggesting that they belong to class III, but this is in contrast to their rather small K_C values mentioned above. Such a class of compounds is regarded as "class IIB" compounds, as discussed by Lapinte [4o].

2.3.3. Substituent effects on p-diethynylbenzene system **3**

The Hammet plot [19], a classical evalution method of the substituent effect, was applied to the series of the *p*-diethynylbenzene system **3**. But the situation is not so simple, because the ethynyl groups are located *ortho* with respect to one substituent but *meta*

Table 2
IVCT bands for the diiron complexes $\mathbf{3}^{+}$–$\mathbf{5}^{+}$.[a]

R	ν_{max} (cm^{-1})	ε ($M^{-1}\,cm^{-1}$)	$\nu_{1/2}$(exp) (cm^{-1})	$\nu_{1/2}$ (cm^{-1})	V^{II}_{ab} (eV)	V^{III}_{ab} [b] (eV)
$\mathbf{3}^{+}\mathbf{a}$	4554	21800	1022	3243	0.070	0.282
$\mathbf{3}^{+}\mathbf{b}$	4570	21600	1310	3249	0.079	0.283
$\mathbf{3}^{+}\mathbf{c}$	4100	17550	1750	3077	0.078	0.254
$\mathbf{3}^{+}\mathbf{d}$[c]	5100	8770	1350	3432	0.054	0.316
$\mathbf{3}^{+}\mathbf{e}$	4150	15500	1250	3096	0.062	0.257
$\mathbf{3}^{+}\mathbf{f}$	4080	13800	1620	3070	0.067	0.253
$\mathbf{4}^{+}$	5055	5400	1300	3417	0.045	0.313
$\mathbf{5}^{+}$	5400	250	1300	3532	0.010	0.335

[a] PF_6 salts analyzed by deconvolution based on three Gaussian curves.
[b] V_{ab} values when assumed as Class III species (see text).
[c] Taken from Ref. [4d].

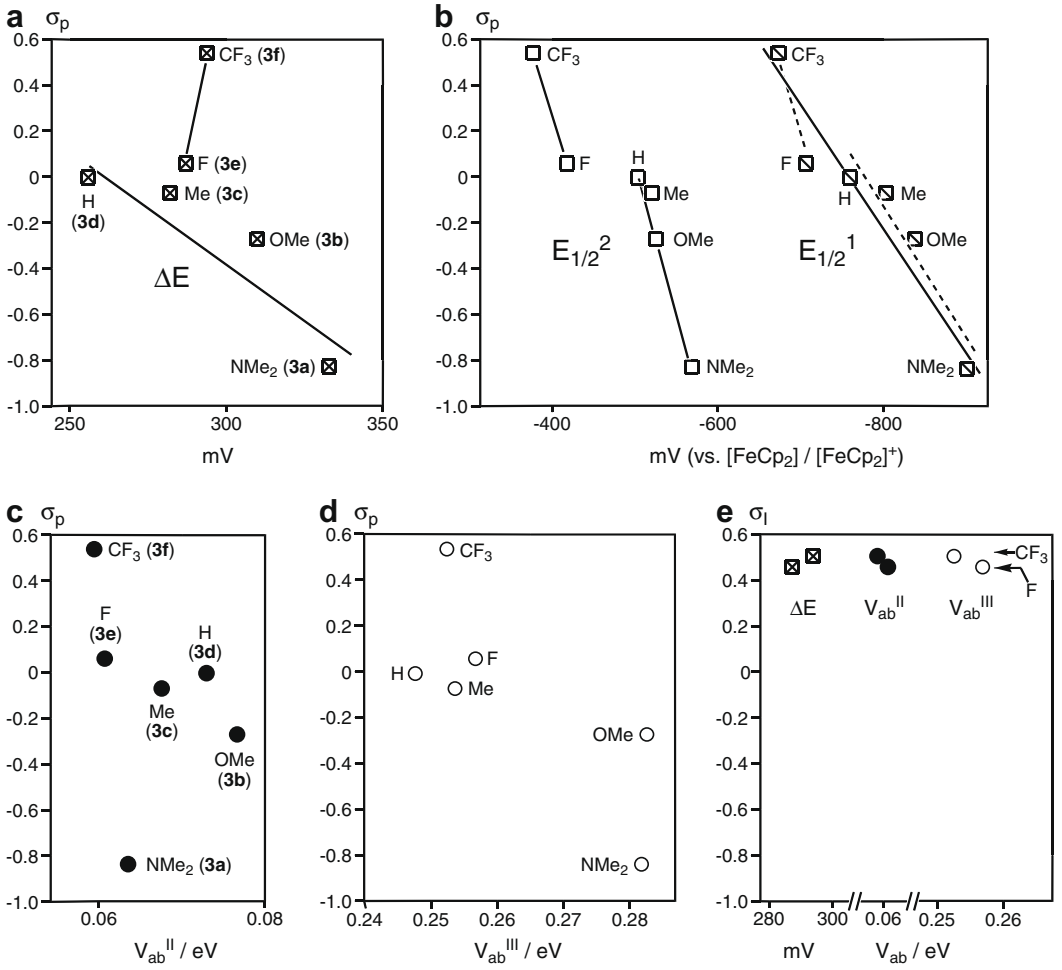

Fig. 2. Plots of (a) ΔE, (b) $E^1_{1/2}$ and $E^2_{1/2}$, (c) V^{II}_{ab}, (d) V^{III}_{ab} for **3** against σ_p, and (e) plots of ΔE, V^{II}_{ab}, and V^{III}_{ab} for **3e,f** against σ_I.

with respect to the other substituent. Furthermore, because σ_o is not defined owing to the steric reason, σ_p is used instead to see the resonance effect of the substituents.

When the $E^1_{1/2}$ values are plotted against σ_p and σ_m, a better fitting is obtained for the former (R^2 = 0.919 (σ_p; solid line in Fig. 2b), 0.775 (σ_m)). This is presumably because (1) the electron-donating substituents employed in this study are the groups with the lone pair electrons on the α-heteroatom (**a**, **b**, and **e**) or the groups only (or mainly) with the σ-inductive effect (**c** and **f**). Substituent effects of such groups can be roughly correlated to σ_p. In other words, (2) electron-withdrawing substituents with the vacant p-orbital at the α-position, which are better described by σ_m, are not included in the present study. The following discussion, therefore, is based on the plots against σ_p. The $E^1_{1/2}$ values for **3a–f** also show a good linear relationship (R^2 = 0.929) with those for the related mononuclear species, *Fe*–C≡C–C_6H_4-X-*p*, reported by Paul and Lapinte [4i,k,n,p].

The linear $E^1_{1/2} - \sigma_p$ correlation (Fig. 2b) indicates that electron-donating substituents facilitate the first oxidation of **3**, as expected.

In contrast to the good fitting of the $E^1_{1/2} - \sigma_p$ plots no apparent linear relationship is noted between σ_p and ΔE (Fig. 2a). When the trend of the second redox potentials $E^1_{1/2}$ (Fig. 2b) is inspected, discontinuity is found between **3d** and **3e**, suggesting that the series of compounds **3a–d** and **3e,f** should be discussed separately. The shifts of $E^2_{1/2}$ for **3e,f** to the anodic side compared to **3a–d** result in increase of the ΔE values eventually leading to the large K_C values.

In order to see the discontinuity issue from another side the performance was evaluated on the basis of the V_{ab} values obtained from the IVCT bands of the monocationic species $\mathbf{3}^+$. The obtained V^{II}_{ab} and V^{III}_{ab} values for them (Table 2) are plotted against σ_p (Fig. 2c and d). Because (1) the differences are very small (ΔV^{II}_{ab} = 0.024 eV; ΔV^{III}_{ab} = 0.063 eV) and (2) the V_{ab} values cannot be determined accurately because of the IVCT bands overlapping with the solvent absorptions, only a trend can be seen from the plots and a rough relationship between the V_{ab} and σ_p values is noted, i.e. electron-donating substituents (with smaller σ_p values) give larger V_{ab} values. In addition, **3e,f** do not always show better performance, as suggested by the CV measurements. The abnormal behavior noted for **3e**,**f** (the large K_C values), therefore, should be due to some other reason.

Abnormal trends as observed for **3e,f** by CV measurements are often ascribed to either destabilization or solvation of the dicationic species $\mathbf{3}^{2+}$ formed by the second oxidation (Scheme 4) [20]. Because, in the present case, (1) only derivatives with the highly σ-electron-withdrawing groups are deviated from the trend and (2) the second oxidation processes of them ($E^2_{1/2}$) are shifted toward the anodic side, the destabilization would be the main reason. When the σ_I and σ^0_R values for the F-containg groups are compared (F: σ_I = 0.50, σ^0_R = −0.35; CF_3: σ_I = 0.45, σ^0_R = 0.01), the inductive effects (σ_I) of the two groups are comparable in contrast to the resonance effects (σ^0_R) being significantly different owing to the presence/absence of lone pair electrons on the atoms adjacent to the aromatic ring. When σ_I is taken as the measure, it is understandable that **3e,f** with the substituents of the similar σ_I values (0.50 (F)/0.45 (CF_3)) give the very similar $E^2_{1/2}$ values (−419 mV (F)/−378 mV (CF_3); Fig. 2e). The V^{II}_{ab} and V^{III}_{ab} plots against σ_I also bring

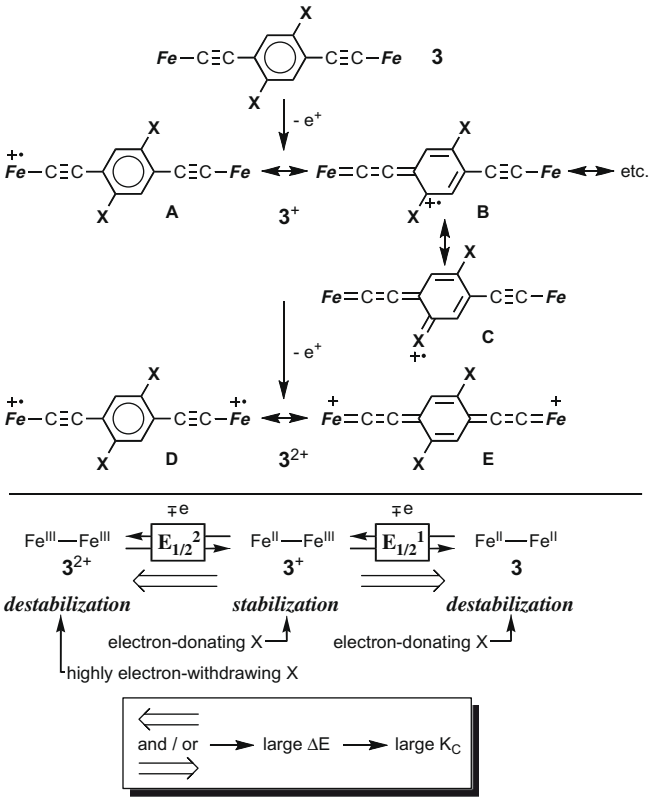

Scheme 4.

the plots for **3e** to the proximity of those of **3f** (Fig. 2e) [18]. The small deviation noted for $E^1_{1/2}$ of **3e** (Fig. 2b) may be also ascribed to this effect, and the situation may be better described by the dotted lines separated into the two series **3a–d** and **3e,f** in a manner similar to the analysis of $E^2_{1/2}$ described above. These considerations suggest that the large K_C values for **3e,f** do not always indicate better performance but result from the inductive effects of the highly σ-electron-withdrawing substituents.

The substituent effects observed by the CV measurements can be interpreted in terms of Scheme 4. As to the shift of $E^1_{1/2}$, electron-donating substituents should increase the electron density at the metal center in the neutral species **3** to make the oxidation easier, i.e. cathodic shift of $E^1_{1/2}$. When attention is turned to the monocationic species $\mathbf{3}^+$ resulting from the 1e-oxidation, the electron-donating substituents in the normal **3a–d** series should stabilize one of the resonance structures **B** with the cation radical center on the aromatic carbon atom adjacent to the substituent (X) through π-interaction with the lone pair electrons on X (**C**) or hyperconjugation with the methyl group (Scheme 4). This effect should cause anodic shift of the second oxidation process ($E^2_{1/2}$). Synergism of these two effects brings about an increase of the ΔE value to be consistent with the results observed.

On the other hand, the highly σ-electron-withdrawing F and CF_3 groups should destabilize the electron-deficient dicationic species $\mathbf{3}^{2+}$ formed by the second oxidation, in particular, through the resonance structure **E**, where the electron-withdrawing X groups directly influence the electronic structures of the Fe moieties to cause lowering the electron densities at the Fe centers. Although similar destabilization is applicable to the monocationic species $\mathbf{3}^+$, the effect should be more serious for the more electron-deficient species $\mathbf{3}^{2+}$ than for $\mathbf{3}^+$. As a result, the ΔE values become larger compared to the other derivatives (Scheme 4). Similar effects were reported for the endiyne system [7] described in Introduction and other systems [20].

Combination of the results of the electrochemical and IVCT measurements leads to the conclusion that, for the *p*-diethynylbenzene system **3**, electron-donating substituents improve the wire-like performance. On the other hand, the large K_C values observed for the derivatives with highly σ-electron-withdrawing groups such as F and CF_3 (**3e,f**) do not reflect the real performance owing to the σ-inductive effects and, therefore, the estimation should be confirmed by taking into account the results of other estimation methods including the IVCT measurement (V_{ab}).

2.4. Other comments

2.4.1. Switching performance of the pH-sensitive derivatives

In addition to the study on molecular wires, more sophisticated functions such as switch are essential for development of molecular circuits [1]. Recently, we reported photoswitchable molecular wires containing the photochromic dithienylethene units [9]. pH-control is another promising switching mechanism and, on the basis of this concept, we planed preparation of compounds **3a** (X = NMe_2) and **3g** (X = OH). The NMe_2 derivative **3a** was obtained successfully, whereas the attempted preparation of **3g** via the vinylidene method resulted in the formation of the cyclized benzodifuran complex **4**, as described above (Scheme 3). Then protonation behavior of **3a** was monitored by CV and IVCT measurements. The CV trace of **3a** in the presence of 1 equivalent of CH_3COOH was similar to that of **3a** with the exception of disappearance of the oxidation wave of the first redox process (Fig. S4), but the IVCT band disappeared upon addition of CF_3COOH (1 equiv.) (Fig. S5), suggesting occurrence of some switching behavior. Subsequent deprotonation with NEt_3 gave the CV trace identical to that of the neutral species **3a**. But these changes did not result from protonation at the NMe_2 moiety but from protonation at the C≡C moiety leading to the cationic vinylidene species, $[Fe{\equiv}C{\equiv}C(H)–C_6H_2(NMe_2)_2–C{\equiv}C–Fe]^+$, i.e. reversion of the formation process of **3a** (Scheme 2), because similar behavior was observed for the other derivatives (e.g. **3d**) without an acid-sensitive functional group (X). Although the mechanism was different from what we anticipated, the acetylide molecular wire **3** turned out to exhibit switching function by the protonation-deprotonation procedures at the *Fe*–C≡C moiety.

2.4.2. Benzodifuran (*4*) and -thiophene complexes (*5*)

Because molecular wires with fused heteroaromatic bridges are rare [2], performance of the benzodifuran complex **4** as molecular wire was examined as compared with the S-analogue **5**, the benzodithiophene complex. The electrochemical and NIR data for them are summarized in Tables 1 and 2, and the original data are included in Figs. S1 and S2. Complexes **4** and **5** showed the K_C values comparable to those of **3** and **4**, in which the two iron centers are separated by the carbon linkages consisting of eight carbon atoms. The effect of the hetero atom, however, is also significant as can be seen from comparison with the S-analogue **5**, which showed the K_C value smaller than that of **4** by a factor of ca. 30. The different performance can be explained by taking into account σ. When the σ_p values for the OH and SH groups are compared, the OH group (−0.37) is more electron-donating than the SH group (0.15), and the difference mainly comes from the resonance effect as is evident from the considerably different σ^0_R values (−0.40 (OH) versus −0.15 (SH); cf. σ_I: 0.25 (OH), 0.25 (SH)). The lone pair electrons on the O atom, the atomic size of which is comparable to that of the carbon atom, should stabilize the C-centered cationic radical effectively through π-donation, as discussed for the **3**-series compounds (Scheme 4).

3. Experimental

3.1. General methods

All manipulations were carried out under an inert atmosphere by using standard Schlenk tube techniques. THF, toluene, pentane (Na–K alloy), CH_2Cl_2, MeCN (P_2O_5), and MeOH ($Mg(OMe)_2$) were treated with appropriate drying agents, distilled, and stored under argon. For the analytical instruments used in the present study, see our previous papers [7]. *Fe*–Cl [21], benzodithiophene [22], and the precursors **1b–e,g** [23] were prepared according to the reported methods, and the synthetic procedures for **1a,f** are included in the Supporting Information. Other chemicals were purchased and used as received.

3.2. Preparation of **3**

As a typical example, the experimental procedures for **3a** are described [4d]. The other derivatives were prepared following essentially the same procedures.

Fe–Cl (580 mg, 0.98 mmol), KPF_6 (167 mg, 0.91 mmol), and **1a** (100 mg, 0.47 mmol) were dissolved in a 9:1 mixture of MeOH–THF (12 mL), and the resultant mixture was stirred for 12 h at room temperature. Removal of the volatiles under reduced pressure, extraction with ether, filtration through a Celite plug, and removal of the solvent under reduced pressure left brown powder (vinylidene intermediate). To the brown intermediate dissolved in THF (35 mL) was added NaOMe (1.4 mmol; prepared from Na and MeOH), and the mixture was stirred for 20 min. After removal of the volatiles under reduced pressure, the product was extracted with toluene and passed through an alumina column. Removal of the solvent under reduced pressure and washing with ether and pentane gave **1a** as red powder (173 mg, 26% yield). **3a**: δ_H (C_6D_6) 1.63 (30H, s, Cp^*), 1.96, 2.91(4H × 2, br × 2, CH_2), 2.60 (12H, s, NMe_2) 6.83 (2H, s, C_6H_2), 8.12–7.10 (40H, m, Ph); δ_P (C_6D_6) 94.2; IR (KBr/ cm^{-1}) ν(C≡C) 2041 cm^{-1}; ESI-MS: 1389 (M+1); Anal. Calc. for $C_{86}H_{92}N_2P_4Fe_2$: C, 77.35; H, 6.67; N, 2.02. Found: C, 73.61; H, 6.51; 1.98%. **3b** (4% yield; red powder): δ_H (C_6D_6) 1.62 (30H, s, Cp^*), 1.98, 2.98 (4H × 2, br × 2, CH_2), 3.46 (6H, s, OMe), 6.70 (2H, s, C_6H_2), 8.16–7.04 (40H, m, Ph); δ_P (C_6D_6) 94.0; ν(C≡C) 2049 cm^{-1}; ESI-MS: 1364 (M+1); Anal. Calc. for $C_{85.5}H_{89}P_4Cl_3Fe_2$ (**3b** · $(CH_2Cl_2)_{1.5}$): C, 68.89; H, 6.02. Found: C, 68.84; H, 6.25%. **3c** (4% yield; red powder): δ_H (C_6D_6) 1.59 (30H, s, Cp^*), 1.89, 2.73 (4H × 2, br × 2, CH_2), 2.31 (6H, s, Me), 6.70 (2H, s, C_6H_2), 8.00–7.12 (40H, m, Ph); δ_P (C_6D_6) 92.9; ν(C≡C) 2039 cm^{-1}; ESI-MS: 1331 (M+1); Anal. Calc. for $C_{85}H_{88}P_4Cl_2Fe_2$ (**3c** · CH_2Cl_2): C, 72.09; H, 6.26. Found: C, 71.87; H, 6.52%. **3e** (9% yield; red powder): δ_H (C_6D_6) 1.54 (30H, s, Cp^*Me), 1.88, 2.76 (4H × 2, br × 2, CH_2), 6.88 (2H, t, J = 8.6 Hz, C_6H_2), 8.07–7.03 (40H, m, Ph); δ_P (C_6D_6) 93.1; ν(C≡C) 2049 cm^{-1}; ESI-MS: 1339 (M+1); Anal. Calc. for $C_{83}H_{82}P_4Cl_2Fe_2$ (**3e** · CH_2Cl_2): C, 70.00; H, 5.80. Found: C, 69.54; H, 5.97%. **3f** (6% yield; red powder): δ_H (C_6D_6) 1.55 (30H, s, Cp^*), 1.90, 2.70 (4H × 2, br × 2, CH_2), 6.88 (2H, s, C_6H_2), 7.94–7.05 (40H, m, Ph); δ_P (C_6D_6) 93.0; ν(C≡C) 2032 cm^{-1}; ESI-MS: 1439 (M+1) [24].

3.3. Preparation of benzodifuran complex **4**

Fe–Cl (672 mg, 1.1 mmol), KPF_6 (198 mg, 1.1 mmol), and **1 g** (85 mg, 0.54 mmol) were dissolved in a 5:4 mixture of MeOH–THF (18 mL), and the resultant mixture was stirred for 14 h at room temperature. Removal of the volatiles under reduced pressure, extraction with CH_2Cl_2, filtration through a Celite plug, and removal of the solvent under reduced pressure left brown powder (the cyclized intermediate **2 g**$'^{2+}$: (δ_H (CD_3CN) 1.34 (30H, s, Cp^*), 2.93, 3.20 (4H × 2, br × 2, CH_2 in dppe), 3.45 (4H, m, CH_2), 5.99 (2H, s, C_6H_2), 7.51–6.96 (40H, m, Ph); δ_H (CD_3CN) 105.1), which was washed with ether and pentane. To the brown intermediate dissolved in THF (30 mL) was added NaOMe (1.2 mmol; prepared from Na and MeOH), and the mixture was stirred for 20 min. After removal of the volatiles under reduced pressure, the product was extracted with toluene and passed through an alumina column. Removal of the solvent under reduced pressure and washing with acetonitrile and pentane gave **4** as red powder (620 mg, 87% yield). **4**: δ_H (C_6D_6) 1.53 (30H, s, Cp^*), 1.85, 2.48 (4H × 2, br × 2, CH_2), 5.86, 6.76 (2H × 2, s × 2, Ar), 7.55–7.08 (40H, m, Ph); δ_P (C_6D_6) 100.3; ESI-MS: 1335 (M+1) [24].

3.4. Formation of the Fischer carbene species $\mathbf{2}^{2+}\mathbf{g}' \cdot [(\mu\text{-}O)(FeCl_3)_2]$ and di-Cp^*-substituted benzodifuran **A** and $[Fe(\kappa_2\text{-dppe})_2(NCMe)_2]^{2+}[(\mu\text{-dppe})\{FeCl_3\}_2]^{2-}$ **B** [12]

Repeated recrystallization of a reaction mixture of **1g**/*Fe*–Cl/KPF_6 from MeCN gave single crystals of $\mathbf{2}^{2+}\mathbf{g}'$ having $[Cl_3Fe\text{–}O\text{–}FeCl_3]^{2-}$ as the counter anion and two more products, the di-Cp^*-substituted benzodifuran **A** and $[Fe(\kappa_2\text{-dppe})_2(NCMe)_2]^{2+}$-$[(\mu\text{-dppe})\{FeCl_3\}_2]^{2-}$ **B**, which were characterized by X-ray crystallography (see Supporting Information). The organic component **A** could be isolated by TLC separation and further characterized by ^1H NMR [δ_H (CD_3CN) 1.35 (6H, s, Me), 0.68, 1.84 (12H × 2, s × 2, Me), 6.39, 7.37 (2H × 2, s × 2, Ar)].

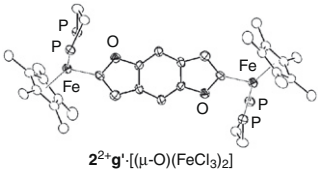

$\mathbf{2}^{2+}\mathbf{g}'\cdot[(\mu\text{-}O)(FeCl_3)_2]$
(Ph and $[(\mu\text{-}O)(FeCl_3)_2]^{2-}$: omitted for clarity)

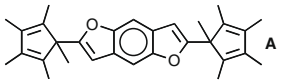

$[Fe(\kappa^2\text{-dppe})_2(NCMe)_2][(\mu\text{-dppe})(FeCl_3)_2]$ **B**

3.5. Preparation of benzodithiophene complex **5**

LDA was prepared by addition of *t*-BuLi (1.57 M in hexane, 1.7 mL, 2.7 mmol) to $HNPr^i_2$ (1.6 mL) dissolved in THF (10 mL) at −78 °C [25]. After stirring for 15 min at the same temperature benzodithiophene [22] (50 mg, 0.26 mmol) dissolved in THF (5 mL) was added dropwise. After further stirring for 30 min I-$FeCp^*(CO)_2$ (1.01 g, 2.7 mmol) was added, and the resultant mixture was stirred for 20 min at −78 °C and then for 2 h at room temperature. The residue obtained by removal of the volatiles under reduced pressure was washed with hexane, extracted with toluene, and filtered through a Celite plug. Removal of the solvent under reduced pressure gave the carbonyl complex, $(CO)_2Cp^*Fe$-benzodithiophene-$FeCp^*(CO)_2$, as yellow powder (36 mg, 20%; δ_H ($CDCl_3$) 1.78 (s, 30H, Cp^*), 6.95, 7.81(2H × 2, s × 2, Ar–H); IR (KBr) ν(CO) 1993, 1939 cm^{-1}). The carbonyl intermediate and dppe (48 mg, 0.12 mmol) were dissolved in toluene–acetonitrile mixture (95:5; 50 mL) and irradiated for 1.5 h. The solution color changed from yellow to orange. Removal of the solvent, extraction with toluene, and filtration through an alumina pad followed by removal of the solvent left red solid, which was washed with pentane and acetonitrile. The product **5** was obtained as red powder (60 mg, 93%

based on the carbonyl intermediate). **5**: δ_H (C_6D_6) 1.56 (30H, s, Cp^*), 1.88, 2.40 (4H × 2, br × 2, CH_2), 6.08 (2H, s, Ar), 7.55–6.98 (42H, m, Ph and Ar); δ_H (C_6D_6) 94.9; ESI-MS: 1366 (M+1) [24].

3.6. Electrochemical measurements

Electrochemical measurements were made with a BAS 100B/W analyzer. CV measurements were performed with a Pt electrode for CH_2Cl_2 solutions of the samples ($\sim 2 \times 10^{-3}$ M) in the presence of an electrolyte ($[Bu_4N \cdot PF_6] = 0.1$ M) at room temperature under an inert atmosphere. The scan rates were 100 mV/s. After the measurement, ferrocene (Fc) was added to the mixture and the potentials were calibrated with respect to the Fc/Fc^+ redox couple (+0.65 V versus Ag/Ag^+ (in CH_2Cl_2)) [14]. Simulation of the electrochemical data was performed with Origin 6.1.

3.7. Preparation of monocationic species

A mixture of **3a** (30 mg, 0.022 mmol) and $[FeCp_2]PF_6$ (6.5 mg, 0.20 mmol) in CH_2Cl_2 (5 mL) was stirred for 15 min at −78 °C and then for 3 h at room temperature. The orange suspended mixture turned into a homogeneous purple solution. After removal of the volatiles under reduced pressure the residue was washed with ether and pentane, and recrystallized from CH_2Cl_2–ether to give $\mathbf{3^+a} \cdot PF_6$ as deep purple powder. The other monocationic species $\mathbf{3^+}$–$\mathbf{5^+}$ were prepared analogously.

Acknowledgments

We are grateful to the Ministry of Education, Culture, Sports, Science and Technology of the Japanese Government and the Japan Society for Promotion of Science and Technology for financial support of this research.

Appendix A. Supplementary material

CCDC 708620, 708621, 708622 contain the supplementary crystallographic data for this paper. These data can be obtained free of charge from The Cambridge Crystallographic Data Centre via www.ccdc.cam.ac.uk/data_request/cif. Supplementary data associated with this article can be found, in the online version, at doi:10.1016/j.jorganchem.2009.01.019.

References

[1] J. Jortner, M.A. Ratner, Molecular Electronics, Blackwell Science, Oxford, 1997;
A. Aviram, M. Ratner, Ann. NY Acad. Sci. (1998) 852;
M. Ratner, Nature 404 (2000) 137;
J.M. Tour, Acc. Chem. Res. 33 (2000) 791;
K.W. Hipps, Science 284 (2001) 536;
D. Cahen, G. Hodes, Adv. Mater. 14 (2002) 789;
R.L. Caroll, C.B. Gorman, Angew. Chem., Int. Ed. Engl. 41 (2002) 4378;
N. Robertson, G.A.Mc. Gowan, Chem. Soc. Rev. 32 (2003) 96;
M.A. Reed, T. Lee (Eds.), Molecular Nanoelectronics, American Scientific Publishers, Stevenson Ranch, CA, 2003;
A.H. Flood, J.F. Stoddart, D.W. Steuerman, J.R. Heath, Science 306 (2004) 2055;
K. Nørgaard, T. Bjørnholm, Chem. Commun. (2005) 1812;
M.C. Petty, Molecular Electronics, From Principles to Practice, Wiley Interscience, New York, 2008.
[2] (b) P.F.H. Schwab, J.R. Smith, J. Michl, Chem. Rev. 105 (2005) 1197;
(a) P.F.H. Schwab, M.D. Levin, J. Michl, Chem. Rev. 99 (1999) 1863.
[3] M.I. Bruce, P.J. Low, Adv. Organomet. Chem. 50 (2004) 231.
[4] (a) F. Paul, C. Lapinte, Coord. Chem. Rev. 178 (1998) 431;
(b) N. Le Narvor, L. Toupet, C. Lapinte, Chem. Commun. (1993) 357;
(c) N. Le Narvor, L. Toupet, C. Lapinte, J. Am. Chem. Soc. 117 (1995) 7129;
(d) N. Le Narvor, C. Lapinte, Organometallics 14 (1995) 634;
(e) N. Le Narvor, C. Lapinte, Compt. Rend. Ser. II Chim. 1 (1998) 745;
(f) M. Guillemot, L. Toupet, C. Lapinte, Organometallics 17 (1998) 1928;
(g) T. Weyland, K. Costuas, A. Mari, J.F. Halet, C. Lapinte, Organometallics 17 (1998) 5569;
(h) S. Le Stang, F. Paul, C. Lapinte, Organometallics 19 (2000) 1035;
(i) R. Denis, L. Toupet, F. Paul, C. Lapinte, Organometallics 19 (2000) 4240;
(j) F. Coat, F. Paul, C. Lapinte, L. Toupet, L. Costuas, J.-F. Halet, J. Organomet. Chem. 683 (2003) 368;
(k) K. Costuas, F. Paul, L. Toupet, J.-F. Halet, C. Lapinte, Organometallics 24 (2005) 2053;
(l) S. Roue, C. Lapinte, T. Bataille, Organometallics 23 (2004) 2558;
(m) F. de Montigny, G. Argouarch, K. Costuas, J.F. Halet, T. Roisnel, L. Toupet, C. Lapinte, Organometallics 24 (2005) 4558;
(n) F. Paul, L. Toupet, J.-Y. Thépot, K. Costuas, J.-F. Halet, C. Lapinte, Organometallics 24 (2005) 5464;
(o) G.S. Ibn, F. Paul, L. Toupet, C. Lapinte, J. Am. Chem. Soc. 128 (2006) 2463;
(p) F. Paul, B.G. Ellis, M.I. Bruce, L. Toupet, T. Roisnel, K. Costuas, J.-F. Halet, C. Lapinte, Organometallics 25 (2006) 649;
(q) F. Paul, S. Goeb, F. Justaud, G. Argouarch, L. Toupet, R.F. Ziessel, C. Lapinte, Inorg. Chem. 46 (2007) 9036;
(r) S. Ibn Ghazala, N. Gauthier, F. Paul, L. Toupet, C. Lapinte, Organometallics 26 (2007) 2308;
(s) S. Szafert, F. Paul, W.E. Meyer, J.A. Gladysz, C. Lapinte, Compt. Rend. Chem. 11 (2008) 693;
(t) F. de Montigny, G. Argouarch, T. Roisnel, L. Toupet, C. Lapinte, S.C.F. Lam, C.H. Tao, V.W.W. Yam, Organometallics 27 (2008) 1912;
(u) C. Lapinte, J. Organomet. Chem. 693 (2008) 793.
[5] M.I. Bruce, P.J. Low, K. Costuas, J.-F. Halet, S.P. Best, G.A. Heath, J. Am. Chem. Soc. 122 (2000) 1949;
M.I. Bruce, B.D. Kelly, B.W. Skelton, A.H. White, J. Organomet. Chem. 604 (2000) 150;
M.I. Bruce, B.G. Ellis, P.J. Low, B.W. Skelton, A.H. White, Organometallics 22 (2003) 3184;
M.I. Bruce, M.E. Smith, B.W. Skelton, A.H. White, J. Organomet. Chem. 637–639 (2001) 484;
See also recent papers,M.I. Bruce, K. Costuas, T. Davin, J.F. Halet, K.A. Kramarczuk, P.J. Low, B.K. Nicholson, G.J. Perkins, R.L. Roberts, B.W. Skelton, M.E. Smith, A.H. White, Dalton Trans. (2007) 5387;
M.I. Bruce, K. Costuas, B.G. Ellis, J.F. Halet, P.J. Low, B. Moubaraki, K.S. Murray, N. Ouddai, G.J. Perkins, B.W. Skelton, A.H. White, Organometallics 26 (2007) 3735;
M.I. Bruce, M.L. Cole, C.R. Parker, B.W. Skelton, A.H. White, Organometallics 27 (2008) 3352;
M.I. Bruce, M. Jevric, C.R. Parker, W. Patalinghug, B.W. Skelton, A.H. White, N.N. Zaitseva, J. Organomet. Chem. 693 (2008) 2915;
M.I. Bruce, N.N. Zaitseva, B.K. Nicholson, B.W. Skelton, A.H. White, J. Organomet. Chem. 693 (2008) 2887;
M.I. Bruce, M. Gaudio, G. Melino, N.N. Zaitseva, B.K. Nicholson, B.W. Skelton, A.H. White, J. Cluster Sci. 19 (2008) 147.
[6] M. Brady, W. Weng, Y. Zhou, J.W. Seyler, A.J. Amoroso, A.M. Arif, M. Bohme, G. Frenking, J.A. Gladysz, J. Am. Chem. Soc. 119 (1997) 775;
T. Bartik, W. Weng, J.A. Ramsden, S. Szafert, S.B. Falloon, A.M. Arif, J.A. Gladysz, J. Am. Chem. Soc. 120 (1998) 11071;
R. Dembinski, T. Bartik, B. Bartik, M. Jaeger, J.A. Gladysz, J. Am. Chem. Soc. 122 (2000) 810;
See also recent publications and references cited therein.Q.L. Zheng, J.A. Gladysz, J. Am. Chem. Soc. 127 (2005) 10508;
S. Szafert, J.A. Gladysz, Chem. Rev. 106 (2006);
PR1.Q.L. Zheng, J.C. Bohling, T.B. Peters, A.C. Frisch, F. Hampel, J.A. Gladysz, Chem. Eur. J. 12 (2006) 6486;
L. de Quadras, F. Hampel, J.A. Gladysz, Dalton Trans. (2006) 2929;
L. de Quadras, E.B. Bauer, J. Stahl, F. Zhuravlev, F. Hampel, J.A. Gladysz, New J. Chem. 31 (2007) 1594;
J. Stahl, W. Mohr, L. de Quadras, T.B. Peters, J.C. Bohling, J.M. Martin-Alvarez, G.R. Owen, F. Hampel, J.A. Gladysz, J. Am. Chem. Soc. 129 (2007) 8282;
L. de Quadras, E.B. Bauer, W. Mohr, J.C. Bohling, T.B. Peters, J.M. Martin-Alvarez, F. Hampel, J.A. Gladysz, J. Am. Chem. Soc. 129 (2007) 8296;
L. de Quadras, J. Stahl, F. Zhuravlev, J.A. Gladysz, J. Organomet. Chem. 692 (2007) 1859;
R.T. Farley, Q.L. Zheng, J.A. Gladysz, K.S. Schanze, Inorg. Chem. 47 (2008) 2955;
J. Stahl, J.C. Bohling, T.B. Peters, L. de Quadrasi, J.A. Gladysz, Pure Appl. Chem. 80 (2008) 459.
[7] M. Akita, Y. Tanaka, C. Naitoh, T. Ozawa, N. Hayashi, M. Takeshita, A. Inagaki, M.-C. Chung, Organometallics 25 (2006) 5261;
Y. Tanaka, T. Ozawa, A. Inagaki, M. Akita, Dalton Trans. (2007) 928;
T. Ozawa, M. Akita, Chem. Lett. (2004) 1180.
[8] M. Akita, T. Koike, Dalton Trans. (2008) 3523.
[9] Y. Tanaka, A. Inagaki, M. Akita, Chem. Commun. (2007) 1169;
K. Motoyama, T. Koike, M. Akita, Chem. Commun. (2008) 5812.
[10] Attempted preparation of, for example, **3a** via Sonogashira coupling between 1,4-dimethylamino-3,5-diiodobenzene and *Fe*–C≡C–H resulted in homocoupling of the latter to give the butadiynediyl complex, *Fe*–C≡C–C≡C–*Fe* [4b,c].
[11] Use of $KOBu^t$ in place of NaOMe lowered the yield of **3**. The low yields of **3** should be due to their low solubility in organic solvents, which should hinder effective extraction.
[12] Formation of **A** and **B** suggests occurrence of coupling of the benzodifuran moiety and the Cp^* ligand. The organic product **A** might result from migratory insertion of the Cp^* ligand to the carbene moiety in $\mathbf{2^{2+}g'}$ followed by deprotonation and demetalation, and the Fe(0) species formed should be

oxidized during the work up and trapped by dppe, Cl^- and MeCN present in the mixture to be converted into **B**.
[13] W. Petz, Iron–Carbene Complexes, Springer, Berlin, 1992.
[14] N.G. Connely, W.E. Geiger, Chem. Rev. 96 (1996) 877;
F. Barriére, W.E. Geiger, J. Am. Chem. Soc. 128 (2006) 3980.
[15] Because of the low solubility of the neutral species **3** in common organic solvents CV measurements were examined for the monocationic species $\mathbf{3}^+$.
[16] N.S. Hush, Prog. Inorg. Chem. 8 (1967) 357;
N.S. Hush, Prog. Inorg. Chem. 8 (1967) 391;
M.B. Robin, P. Day, Adv. Inorg. Chem. Radiochem. (1967) 247.
[17] R.C. Rocha, F.N. Rein, H. Jude, A.P. Shreve, J.J. Concepcion, T.J. Meyer, Angew. Chem., Int. Ed. 47 (2008) 503.
[18] Plots of ΔE, $E^1_{1/2}$, and $E^2_{1/2}$ data against σ_I and σ^0_R are shown in Fig. S3.
[19] C. Hansch, S. Leo, R.W. Taft, Chem. Rev. 91 (1991) 165.
[20] M.-C. Chung, X. Gi, B.A. Etzenhouser, A.M. Spuches, P.T. Rye, S.K. Seetharaman, D.J. Rose, J. Zubieta, M.B. Sponsler, Organometallics 22 (2003) 3485.
[21] C. Roger, P. Hamon, L. Toupet, L. Rabaa, J.-Y. Saillard, J.-R. Hamon, C. Lapinte, Organometallics 10 (1991) 1045.
[22] K. Tamiya, Y. Konda, H. Ebata, N. Niihara, T. Otsubo, J. Org. Chem. 70 (2005) 10569.
[23] **1b** T.B. Marder, New J. Chem. 27 (2003) 140;
1cS. Takahashi, Y. Kuroyama, K. Sonogashira, N. Hagihara, Synthesis (1980) 627;
diiodo precursorJ.R. Perry, D.B. Wilson, Macromolecules 28 (1995) 3509;
1dM.J. Plater, J.P. Sinclair, S. Aiken, T. Gelbrich, M.B. Hursthouse, Tetrahedron 60 (2004) 6385;
D.L. Mattern, J. Org. Chem. 49 (1984) 3051;
1eT.X. Neenan, G.M. Whitesides, J. Org. Chem. 53 (1988) 2489;
1gG.T. Crisp, T.P. Bubner, Tetrahedron 53 (1997) 11899.
[24] Despite several attempts analytically pure samples could not be obtained.
[25] LDA prepared from *n*-BuLi gave a low yield mixture of products.